Effects of Electric and Magnetic Charges on Weak Deflection Angle and Bounding Greybody of Black Holes in Nonlinear Electrodynamics

Wajiha Javed,[1,*] Mehak Atique,[1,†] and Ali Övgün[2,‡]

[1]*Department of Mathematics, Division of Science and Technology, University of Education, Lahore-54590, Pakistan*

[2]*Physics Department, Eastern Mediterranean University, Famagusta, 99628 North Cyprus via Mersin 10, Turkey.*

(Dated: June 30, 2022)

Abstract

In this paper, we study the weak deflection angle using Gauss-Bonnet theorem and bounding greybody factor for electric and magnetic black holes in the background of nonlinear electrodynamics. Using Gibbons and Werner's approach, first we acquire the Gaussian optical curvature to use in Gauss-Bonnet theorem and calculate the bending angle for spherically symmetric electric and magnetic black holes in both non-plasma and plasma mediums in the weak field limits. Later, we calculate the rigorous bounds of the greybody factor for the given black holes. Furthermore, we look into the graphical behaviour of bending angles and greybody bounds at some specific values of multiple parameters as well as black holes charges. It is to be mention here that all the results for the electric and magnetic charged black holes solutions reduce into the Schwarzschild black hole solution in the absence of the black holes charges.

PACS numbers: 95.30.Sf, 98.62.Sb, 97.60.Lf

Keywords: gravitational lensing; black holes; Gauss-Bonnet theorem; plasma medium; greybody factor; non-linear electrodynamics

*Electronic address: wajiha.javed@ue.edu.pk

†Electronic address: mehakatique1997@gmail.com

‡Electronic address: ali.ovgun@emu.edu.tr

Preprints (www.preprints.org) | NOT PEER-REVIEWED | Posted: 5 July 2022 doi:10.20944/preprints202202.0245.v2

I. INTRODUCTION

One of the most fascinating objects in the universe is a black hole (BH). The presence of a BH has remained the subject of interest since Einstein found their existence using his theory of general relativity (GR). A BH provides a significant tool to examine and test the essential laws of the universe. A BH is an area in the universe that has such an excessive gravity that nothing can get away from its pull, even the light can not escape. In addition, the first picture of a BH was seen by Event Horizon Telescope collaboration [1, 2].

The concept of gravitational lensing (GL) was first presented by Soldner in 1801 in the background of Newton's theory of gravitation [3]. Einstein declared the presence of gravitational waves and GL as a phenomena of GR in 1916 [4]. The gravitational waves from BHs and neutron stars merger had been recognized via LIGO in 2015, which proved that the theoretical expectancies are nicely geared up with the experimental studies [5, 6]. After the identification of the gravitational waves, a large wide variety of gravity theories faced many drawbacks, but the identification of the gravitational waves also grabbed the attention in the field of GL [7]. Gravitational lensing is extremely useful technique to understand the knowledge of galaxies and universe. Gravitational lensing is a bending of light within the extent of the gigantic objects which is proposed by the GR.

In literature GL has been divided into three types (i) strong GL (ii) weak GL and (iii) micro GL [8]-[13]. Strong GL is the effect of GL which is strong enough to produce multiple images, arc or Einstein's rings, in strong GL geometry is favourable and the bending is comparatively large. In weak GL, the lens is not strong enough to produce the multiple images. Also, in case of weak lensing, the geometry is less favourable. For micro GL, lens is a small mass and the the geometry is extremely favourable and the bending, distortion and multiple images caused by lensing cannot be resolved. The study of GL has gained much attention from researchers and has proved to be very useful to investigate many astrophysical objects like naked singularities, BHs and the wormholes [8]-[60].

In past years, many investigations have connected GL with the Gauss-Bonnet theorem (GBT) after Gibbons and Werner confirmation about the feasible manner to calculate the bending angle of BHs that shows asymptotic behaviour [22]. The bending angle can be defined as:

$$\alpha = -\int\int_{D_\infty} \mathcal{K} dS,$$

where α is representing the bending angle, $\mathcal{K}$ is representing the optical Gaussian curvature, dS represents optical surface and D_∞ indicates the infinite domain of the space. Werner extended

Preprints (www.preprints.org) | NOT PEER-REVIEWED | Posted: 5 July 2022 doi:10.20944/preprints202202.0245.v2

this technique for stationary BHs using Kerr-Randers optical geometry [23]. Recently, Gallo and Crisnejo [24] examined the bending of light in the plasma medium by using GBT. A lot of work has been done through the method of Gibbons and Werner by using GBT [25]-[76].

In 1974, Hawking proved that BHs are indeed grey because of the thermal radiation emitted by the BHs due to the relativistic quantum effects. These radiation are known as Hawking radiation named after British Physicist Stephen Hawking [77]. In the background of quantum field theory the creation and annihilation of the particles is theoretically possible. When pair production occurs near the BH's horizon, one of the particles from the pair falls and the other particles exit from the BH's horizon, particles which exit, these are detected as Hawking radiation by outside observer. On the other hand, according to the GR, BH bends spacetime around itself. For the Hawking radiation, this spacetime acts as a gravitational potential. As a result, the Hawking radiation are passed through this potential. Some of the Hawking radiation reflected back to the BH and other Hawking radiation are transmitted out of the BH to spatial infinity. In this case, the transmission probability is known as the $greybody factor$ [78]-[86]. Higher the value of greybody factor expresses higher probability that Hawking radiation can reach infinity. Some find the greybody factor by using different methods such as WKB approximation and matching technique. In addition, a novel technique for calculating the greybody factor without using approximations has been created which demands the determination of the greybody factor bound [87]-[97].

One of the most major issue from the beginning of the universe is singularity [98]-[103]. In GR, the spacetime singularities boost a whole lot of problems [104]-[110]. In order to eliminate the spacetime singularities occur at the centre of charged BHs different techniques such as nonlinear electrodynamics (NLED) and gravity modification etc have been introduced. Initially, to solve the point-like charge self-energy divergences, the theory of NLED was introduced by Born and later, with the help of Infield this theory was modified and become the Born and Infield theory [121]. In recent years, NLED models have attracted a lot of attention with significant focus on their capacity to find regular BH solutions. In the context of GR paired with a particular NLED model, Bronnikov discovered a class of magnetically charged regular BHs [110]. Kruglov proposed one greater version of NLED with two parameter, where the particular extent of magnetic field, the unitary rules and causality are satisfied [105]. A lot of work has also been done on the consequences of NLED on GL [105]-[119].

In this paper, we work for another model of NLED proposed in [120], i.e., the static spherically symmetric electric and magnetic BH solutions. We examine the astrophysical phenomenon of

Preprints (www.preprints.org) | NOT PEER-REVIEWED | Posted: 5 July 2022 doi:10.20944/preprints202202.0245.v2

bending of light for electric and magnetic BH solutions and examine the effects of NLED on GL and on the bonds of the greybody factor.

This paper is structured as follows. In section **2**, we look over the NLED model and analyze the solution of magnetic and electric BHs and then we find the optical geometry of the magnetic and electric BHs and then we discuss about GBT in detail and find the bending angle of BHs in non-plasma medium. In section **3**, we analyze graphically the bending angle in the non-plasma medium. Section **4**, consists of the computation of the bending angle in plasma medium for magnetic and electric BHs. In section **5**, we discuss the graphical behaviour of the bending angles in plasma medium. Section **6**, consists of to calculate the bounds of greybody factor for electric and magnetic BHs and then in the section **7**, we look into the graphical behaviour of greybody bounds. Section **8** is devoted to conclude the discussion about the results obtained from our analysis.

II. WEAK GRAVITATIONAL LENSING IN NON-PLASMA MEDIUM FOR ELECTRIC AND MAGNETIC BLACK HOLES

The action of the Einstein NLED theory has the form [120]

$$S=\int d^4x\sqrt{-g}\left(\frac{1}{2\kappa^2}\mathcal{R}+\mathcal{L}(\mathcal{F})\right), \tag{1}$$

where $\mathcal{R}$ is the Ricci scalar and $\kappa^2=8\pi G$, where G is the Newton's constant in four dimensional spacetime and $\mathcal{L}=-\frac{1}{\beta}\ln\left(\cos^2\left(\sqrt{-\beta\mathcal{F}}\right)\right)$, where β is a constant with dimension $(length)^4$, $\mathcal{F}=\frac{1}{4}F_{\mu\nu}F^{\mu\nu}$ and $F_{\nu\mu}=\partial_\mu A_\nu-\partial_\nu A_\mu$, Eq.(1) implies the Einstein field equations as

$$\mathcal{R}_{ij}-\frac{1}{2}g_{ij}\mathcal{R}=-\kappa^2T_{ij}, \tag{2}$$

where $\mathcal{R}_{ij}$ is the Ricci tensor. By varying Eq.(1), we determine the equation of motion for electromagnetic field

$$\partial_c(\sqrt{-g}(F^{ij}\mathcal{L}_F+\tilde{F}^{ij}\mathcal{L}_F))=0, \tag{3}$$

where, $\mathcal{L}_F=\frac{\partial\mathcal{L}}{\partial\mathcal{F}}=-\frac{\tan\sqrt{-\beta\mathcal{F}}}{\sqrt{-\beta\mathcal{F}}}$. In our analysis, we consider the static electric and magnetic BH solutions by applying equation of motion for electromagnetic field and Einstein field equations. Kruglov has observed magnetically charged BH in the context of NLED [105], while electrically charged BH solution is observed by Mazharimousavi and Halilsoy [104], and to solve the corresponding Einstein nonlinear Maxwell equations, the invariant is $(\mathcal{F}=-\frac{E^2}{2}=-\frac{q^2}{2r^4})$, where q is the electric charge and for magnetic BH the invariant is $(\mathcal{F}=\frac{B^2}{2}=-\frac{p^2}{2r^4})$, where p is the

Preprints (www.preprints.org) | NOT PEER-REVIEWED | Posted: 5 July 2022 doi:10.20944/preprints202202.0245.v2

magnetic charge. Mazharimousavi and Halilsoy in their new model [120] have examined the static electric and magnetic solutions separately.

A. Optical Metric for Electric Black Hole

The line-element for the electric and magnetic BHs in a static and spherically symmetric space-time is defined by [120]

$$ds^2 = -f(r)dt^2 + \frac{dr^2}{f(r)} + r^2 d\Omega^2, \quad d\Omega^2 = d\theta^2 + \sin^2\theta d\varphi^2, \tag{4}$$

where the metric function $f(r)$ for electric BH is defined as

$$f(r) = 1 - \frac{2GM}{r} - \frac{\pi q^2 G}{2r_o^2} + \mathcal{O}(r^2 lnr) \qquad r \to 0, \tag{5}$$

where q is the electric charge of a BH, M is the real ADM mass of the BH and r_o is the parameter. Supposing the spectator and source both are in a tropical plane and additionally, null photon with the $(\theta = \frac{\pi}{2})$ inside the similar plane, we get optical space as

$$ds^2 = -f(r)dt^2 + \frac{dr^2}{f(r)} + r^2 d\varphi^2. \tag{6}$$

For equatorial plane and the null geodesics $(ds = 0)$, we obtain

$$dt^2 = \frac{dr^2}{(f(r))^2} + \frac{r^2 d\varphi^2}{f(r)}. \tag{7}$$

The non-zero Christoffel symbols of Eq.(7) are calculated as

$$\Gamma^0_{00} = -\frac{f'(r)}{f(r)},$$

$$\Gamma^1_{10} = \frac{1}{r} - \frac{f'(r)}{2f(r)},$$

$$\Gamma^0_{11} = \frac{-2f(r)}{r} + f'(r), \tag{8}$$

in which 0 and 1 indicate r-coordinate and φ-coordinate and the Ricci scalar of the optical metric is computed as

$$\mathcal{R} = f(r)f''(r) - \frac{(f'(r))^2}{2}. \tag{9}$$

Preprints (www.preprints.org) | NOT PEER-REVIEWED | Posted: 5 July 2022 doi:10.20944/preprints202202.0245.v2

Hence, the Gaussian optical curvature is evaluated as

$$\mathcal{K} = \frac{\mathcal{R}}{2}. \tag{10}$$

The Gaussian optical curvature of electric BH in leading order term after calculating and putting the value of $\mathcal{R}$ in Eq.(10) is calculated as

$$\mathcal{K} \simeq -\frac{2GM}{r^3} + \frac{G^2 M \pi q^2}{r_o^2 r^3} + \mathcal{O}(M^2, q^4). \tag{11}$$

B. Bending Angle for Electric Black Hole

Here, we use GBT to obtain the bending angle of electric BH, via GBT to the domain $\mathcal{M}_C$, given as [22]:

$$\int\int_{\mathcal{M}_C} \mathcal{K} dS + \oint_{\partial \mathcal{M}_C} k dt + \sum_l \epsilon_l = 2\pi \mathcal{X}(\mathcal{M}_C), \tag{12}$$

wherein, k indicates the geodesic curvature, written as $k = \breve{g}(\nabla_{\dot{\zeta}} \dot{\zeta}, \ddot{\zeta})$ so that the $\breve{g}(\dot{\zeta}, \dot{\zeta}) = 1$, $\ddot{\zeta}$ symbolizes the unit acceleration vector and external angle of l^{th} vertex symbolizes as ϵ_l. We get the jump angles equal to $\frac{\pi}{2}$, as $\mathcal{C}$ goes to infinity, hence we obtain $\epsilon_l + \epsilon_{ll} \to \pi$. Here, Euler characteristic $\mathcal{X}(\mathcal{M}_C)$ is 1 as the region $\mathcal{M}_C$ is non-singular. So

$$\int\int_{\mathcal{M}_C} \mathcal{K} dS + \oint_{\partial \mathcal{M}_C} k dt + \epsilon_l = 2\pi \mathcal{X}(\mathcal{M}_C), \tag{13}$$

where, $\epsilon_l = \pi$ represents the entire jump angle and $\alpha_{\tilde{g}}$ is geodesic, as the Euler characteristic number is indicated by $\mathcal{X}$ is 1. As $C \to \infty$, the most effective element is to be find as $k(F_C) = |\nabla_{\dot{F}_C} \dot{F}_C|$. The radial component for the sake of the geodesic curvature is defined as [22]:

$$(\nabla_{\dot{F}_C} \dot{F}_C)^r = \dot{F}_C^{\varphi} \partial_{\varphi} \dot{F}_C^r + \Gamma^r_{\varphi\varphi} (\dot{F}_C^{\varphi})^2. \tag{14}$$

For very large C, $F_C := r(\varphi) = C = const.$ Thus, Eq.(14) becomes $(\dot{F}_C^{\varphi})^2 = \frac{1}{(f(r))^2}$. Recalling $\Gamma^r_{\varphi\varphi} = \frac{-2f(r)}{r} + f'(r)$, yields that

$$(\nabla_{\dot{F}_C^r} \dot{F}_C^r)^r \to \frac{-1}{C}. \tag{15}$$

This shows that geodesic curvature does not depend upon the topological defects so, $k(F_C) \to \frac{1}{C}$, but from the Eq.(7) we can write $dt = C d\varphi$. We can obtain this;

$$k(F_C) dt = \frac{1}{C} C d\varphi. \tag{16}$$

Preprints (www.preprints.org) | NOT PEER-REVIEWED | Posted: 5 July 2022 doi:10.20944/preprints202202.0245.v2

By taking into consideration all above equations, we get

$$\int\int_{\mathcal{M}_C} \mathcal{K} ds + \oint_{\partial \mathcal{M}_C} k dt \overset{R\to\infty}{=} \int\int_{W_\infty} \mathcal{K} dS + \int_0^{\pi+\alpha} d\varphi. \tag{17}$$

Supposing that at zeroth order in the weak bending domain the light ray obeys the straight-line approximation which is defined as $r = \frac{b}{\sin\varphi}$. Then, the bending angle can be obtained by using the Eq.(12) and (17) as follows

$$\alpha = -\int_0^{\pi} \int_{\frac{b}{\sin\varphi}}^{\infty} \mathcal{K}\sqrt{det\breve{g}} dr d\varphi, \tag{18}$$

where

$$\sqrt{det\breve{g}} = r(1 + \frac{3GM}{r} + \frac{3q^2\pi G}{4r_o^2}). \tag{19}$$

After putting the Gaussian curvature obtained in Eq.(11) upto the leading terms and Eq.(19) into Eq.(18), the bending angle for electric BH is computed as

$$\alpha \simeq \frac{4GM}{b} + \frac{G^2 M\pi q^2}{r_o^2 b} + \mathcal{O}(M^2, q^4). \tag{20}$$

The obtained bending angle (20) depends on the electric charge q, mass of the BH, parameter r_o and impact parameter b. It is to be mention here that the bending angle α of electric BH in non-plasma medium reduces to Schwarzschild BH bending angle in non-plasma medium upto the order one of M if we neglect the electric charge q.

C. Optical Metric for Magnetic Black Hole

In order to compute the Gaussian optical curvature for magnetic BH, the spherically symmetric metric for the magnetic BH is defined by Eq.(4), where the metric function for the magnetic BH [120] is given as follows

$$f(r) = 1 - \frac{2GM}{r} + \frac{Gp^2}{r^2} - \beta\frac{Gp^4}{60r^6} + \mathcal{O}(r^{-10}) \qquad r \to \infty, \tag{21}$$

where p is the magnetic charge and β is the parameter. After applying the basic procedure, the optical space in equatorial plane ($\theta = \frac{\pi}{2}$) and for the null geodesic ($ds^2 = 0$), we get the optical metric for the magnetic BH as follows:

$$dt^2 = \frac{dr^2}{(1 - \frac{2GM}{r} + \frac{Gp^2}{r^2} - \beta\frac{Gp^4}{60r^6})^2} + \frac{r^2 d\varphi^2}{(1 - \frac{2GM}{r} + \frac{Gp^2}{r^2} - \beta\frac{Gp^4}{60r^6})}. \tag{22}$$

Preprints (www.preprints.org) | NOT PEER-REVIEWED | Posted: 5 July 2022 doi:10.20944/preprints202202.0245.v2

The Gaussian optical curvature is defined in Eq.(10), by computing the Ricci scalar of the optical metric Eq.(22), the Gaussian optical curvature upto the leading order term of magnetize BH is calculated as

$$\mathcal{K} \simeq -\frac{2GM}{r^3} + \frac{3Gp^2}{r^4} - \beta\frac{7Gp^4}{20r^8} + \mathcal{O}(G^2, M^2). \tag{23}$$

D. Bending Angle for Magnetic Black Hole

In this segment, we are interesting in calculating the bending angle for magnetic BH by using GBT in non-plasma medium just as we calculated for electric BH in section (2.2). For obtaining the angle in weak bending limit, as the shaft of light chases the estimation for a straight line so by utilizing $r(t) = b/\sin\varphi$ at zeroth order

$$\alpha = -\int_0^{\pi}\int_{b/\sin\varphi}^{\infty} \mathcal{K}\sqrt{det\breve{g}}drd\varphi, \tag{24}$$

where

$$\sqrt{det\breve{g}}dv = r(1 + \frac{3GM}{r} - \frac{3p^2G}{2r^2} + \beta\frac{Gp^4}{40r^6})dr. \tag{25}$$

By putting the value of $\mathcal{K}$ obtained in Eq.(23) and Eq.(25) in Eq.(24), the bending angle in non-plasma medium for magnetic BH is calculated as

$$\alpha \simeq \frac{4GM}{b} - \frac{3Gp^2\pi}{4b^2} + \beta\frac{7Gp^4\pi}{384b^6} + \mathcal{O}(G^2, M^2). \tag{26}$$

The obtained bending angle (26) depends on the magnetic charge p, mass of the black hole, parameter β and impact parameter b. We also observe that the bending angle α of magnetic BH in non-plasma medium reduces to Schwarzschild BH bending angle in non-plasma medium upto the order one of M if we neglect the magnetic charge p.

III. GRAPHICAL ANALYSIS OF BENDING ANGLES IN NON-PLASMA MEDIUM

This section is devoted to the study of the behaviour of bending angles of electric and magnetic BHs in non-plasma medium graphically and to explain the effect of electric charge q, impact parameter b and parameter r_o (in case of electric BH) and magnetic charge p, impact parameter b and the parameter β (in case of magnetic BH) on the deflection angles.

Preprints (www.preprints.org) | NOT PEER-REVIEWED | Posted: 5 July 2022 doi:10.20944/preprints202202.0245.v2

A. For Electric Black Hole

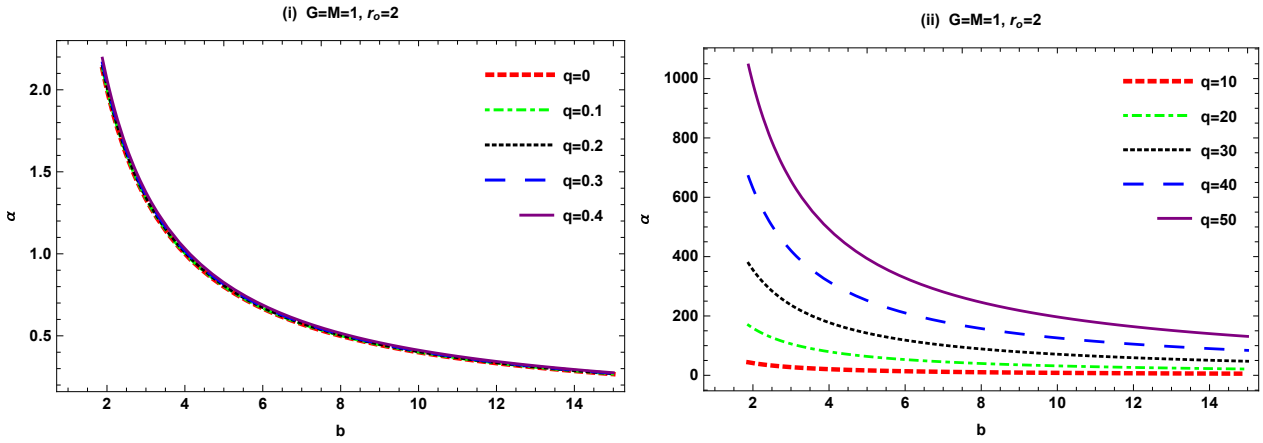

Figure 1: α versus b.

- **Figure 1** demonstrates the graphical behaviour of the bending angle α of electric BH with respect to the impact parameter b for the fixed value of M, G and r_o.

  (i) For the small values of q graph between the the bending angle α and the impact parameter b shows that the behaviour of the bending angle α is uniformly constant.

  (ii) For the large values of q graph between the the bending angle α and the impact parameter b depicts that the behaviour of the bending angle α is increasing gradually.

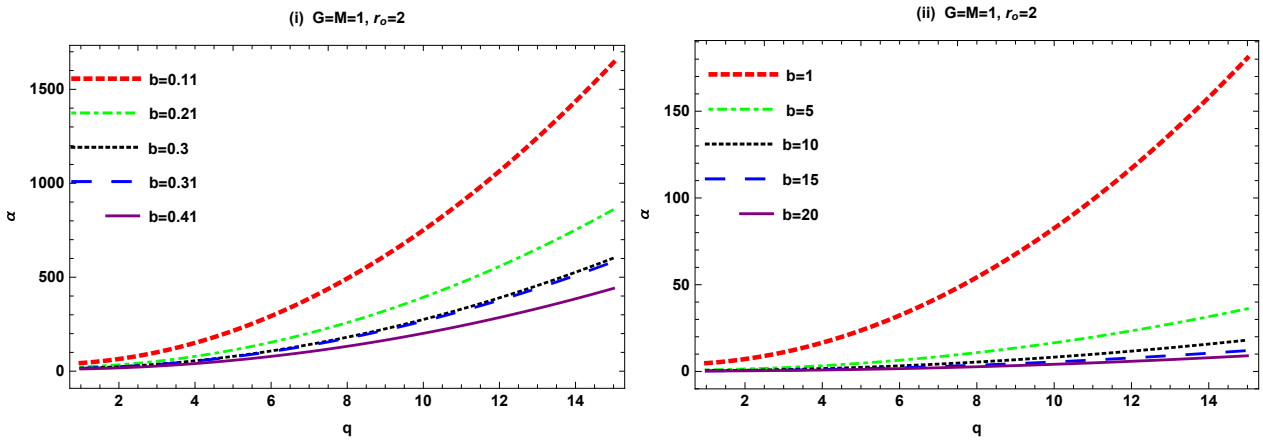

Figure 2: α versus q.

- **Figure 2** exhibits the graphical behaviour of the bending angle α of electric BH with respect to the electric charge q by setting M, G and r_o fixed.

Preprints (www.preprints.org) | NOT PEER-REVIEWED | Posted: 5 July 2022 doi:10.20944/preprints202202.0245.v2

(i) For the small values of impact parameter b the graph of bending angle α with respect to electric charge q exhibits that bending angle α shows decreasing behaviour.

(ii) For the large values of impact parameter b the graph of bending angle α with respect to electric charge q shows that for the values of $1 < b < 5$ bending angle α increasing but as the value of b increasing the behaviour of the bending angle starts decreasing.

B. For Magnetic Black Hole

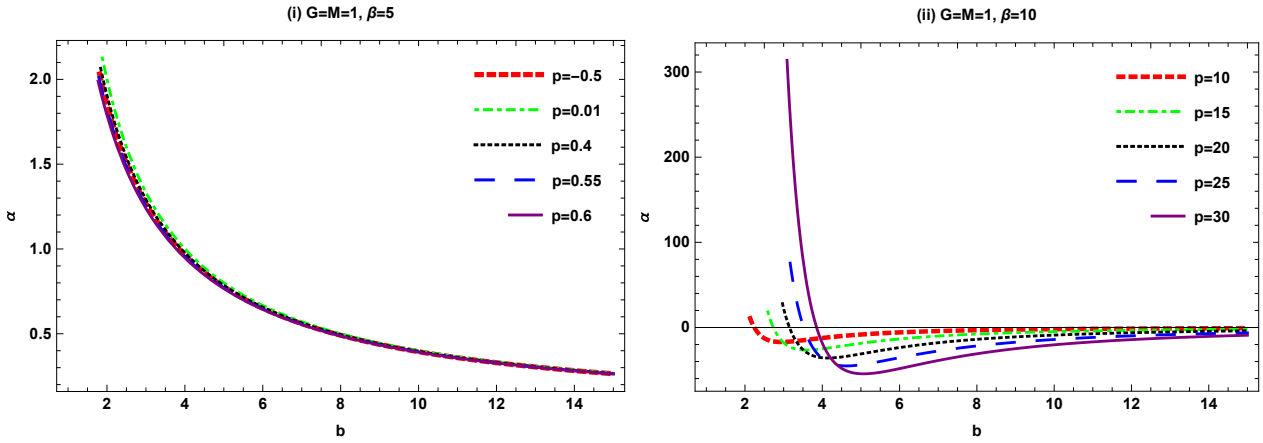

Figure 3: α versus b.

- **Figure 3** exhibits the graphical behaviour of bending angle α of magnetic BH with respect to the impact parameter b for the fixed value of M, G and β.

  (i) Graph between bending angle α and impact parameter b shows that for the very small variation of magnetic charge p and parameter $\beta = 5$ the bending angle α rapidly decreases.

  (ii) Graph between bending angle α and impact parameter b depicts that for the large value of magnetic charge p and parameter $\beta = 10$, the bending angle α increasing and then goes to infinity.

Preprints (www.preprints.org) | NOT PEER-REVIEWED | Posted: 5 July 2022 doi:10.20944/preprints202202.0245.v2

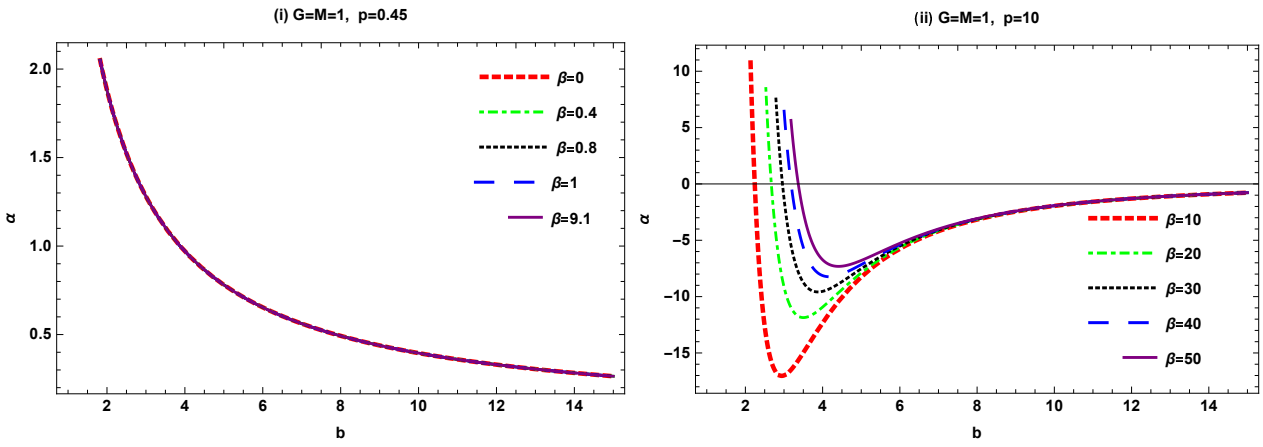

Figure 4: α versus b.

- **Figure 4** represents the graphical behaviour of bending angle α of magnetic BH with respect to the impact parameter b for the fixed value of magnetic charge p, G and M.

  (i) Graph between the bending angle α and impact parameter b exhibits that for small values of parameter β and magnetic charge $p = 0.45$ the bending angle α decreasing constantly.

  (ii) Graph between the bending angle α and impact parameter b exhibits that for the large values of parameter β and magnetic charge $p = 10$ the bending angle α firstly starts decreasing negatively and then increasing and goes to the infinity.

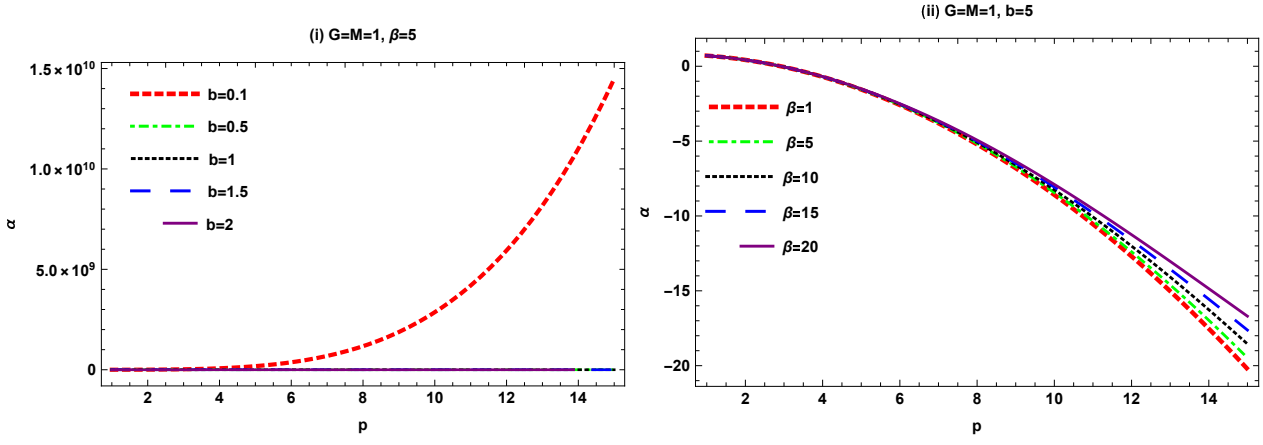

Figure 5: α versus p.

- **Figure 5** demonstrates the graphical behaviour of bending angle α of magnetic BH with respect to the magnetic charge p for the fixed value of G and M.

Preprints (www.preprints.org) | NOT PEER-REVIEWED | Posted: 5 July 2022 doi:10.20944/preprints202202.0245.v2

(i) Graph between the bending angle α and magnetic charge p shows that for the variation of impact parameter b and parameter $\beta = 5$ firstly the bending angle α increases then start decreasing.

(ii) Graph between the bending angle α and magnetic charge p for the variation in the value of parameter β and impact parameter $b = 5$ shows that the bending angle α is negatively increasing.

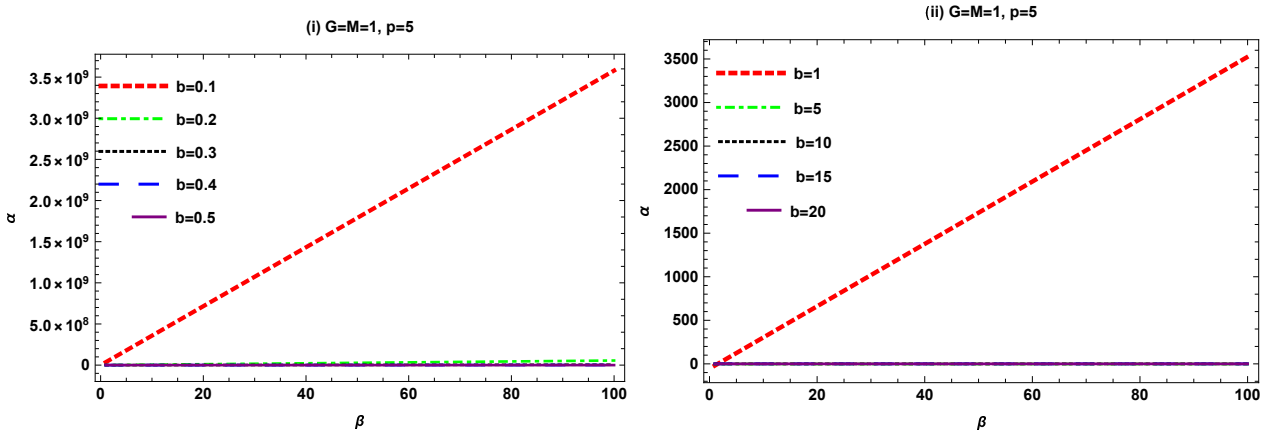

Figure 6: α versus β.

- **Figure 6** represents the graphical behaviour of bending angle α of magnetic BH with respect to the β and keeping magnetic charge p, G and M fixed.

  (i) Graph between the bending angle α and β exhibits that for the small variation of the impact parameter b and magnetic charge $p = 5$ the bending angle α is decreasing.

  (ii) Graph between the bending angle α and β for the large value of impact parameter b and magnetic charge $p = 5$ the bending angle α is decreasing.

IV. INFLUENCE OF PLASMA MEDIUM ON WEAK LENSING

This section is devoted to the study of the impact of plasma medium on the weak lensing. The refractive index for the electric and magnetic BHs is given as [24]

$$\dot{n^2}\left(r, \omega(r)\right) = 1 - \frac{\omega_e^2(r)}{\omega_\infty^2(r)}. \tag{27}$$

Preprints (www.preprints.org) | NOT PEER-REVIEWED | Posted: 5 July 2022 doi:10.20944/preprints202202.0245.v2

A. Optical Metric and Bending Angle for Electric Black Hole

The refractive index for the case of electric BH is given by

$$n(r) = \sqrt{1 - \frac{\omega_e^2}{\omega_\infty^2}\left(1 - \frac{2GM}{r} - \frac{\pi q^2 G}{2r_o^2}\right)}, \tag{28}$$

where ω_e indicates the electron plasma frequency and ω_∞ indicates light frequency computed by the viewer at infinity. The static spherically symmetric metric and the metric function is define as

$$ds^2 = -f(r)dt^2 + \frac{dr^2}{f(r)} + r^2(d\theta^2 + \sin^2\theta d\varphi^2), \tag{29}$$

and

$$f(r) = 1 - \frac{2GM}{r} - \frac{\pi q^2 G}{2r_o^2}. \tag{30}$$

To get optical measurement, by considering light source and the spectator likewise null photon are in the tropical plane with $(\theta = \frac{\pi}{2})$. Now, for null geodesic put $ds^2 = 0$, we get

$$dt^2 = g_{mw}^{opt} dx^m dx^w = n^2 \left[\frac{dr^2}{f^2(r)} + \frac{r^2 d\varphi^2}{f(r)}\right], \tag{31}$$

with determinant g_{mw}^{opt},

$$\sqrt{g^{opt}} = r\left(1 - \frac{\omega_e^2}{\omega_\infty^2}\right) + GM\left(3 - \frac{\omega_e^2}{\omega_\infty^2}\right) + \frac{\pi q^2 G r}{4r_o^2}\left(3 - \frac{\omega_e^2}{\omega_\infty^2}\right). \tag{32}$$

The non-zero Christoffel Symbols by using Eq.(31) are calculated as

$$\Gamma_{00}^0 = \frac{(f(r)\omega_e^2 - 2\omega_\infty^2)(f(r)\omega_e^2 + \omega_\infty^2)f'(r)}{2f(r)\omega_\infty^4},$$

$$\Gamma_{10}^1 = \frac{r}{2}\left(\frac{(f(r))^3\omega_e^4}{\omega_\infty^4} + rf'(r) - 2f(r) + \frac{r\omega_e^2 f'(r)}{\omega_\infty^2}f(r)\right),$$

$$\Gamma_{11}^0 = \frac{1}{r} - \frac{(f(r))^2\omega_e^4}{r\omega_\infty^4} - \frac{f'(r)}{2f(r)},$$

where 0 and 1 indicate r-coordinate and φ-coordinate. The $\mathcal{K}$ can be obtained by utilizing the above Christoffel symbols as

$$\mathcal{K} = \frac{R_{r\varphi r\varphi}(g^{opt})}{det(g^{opt})}, \tag{33}$$

with the help of Eq.(33), the $\mathcal{K}$ for the electric BH is computed as

$$\mathcal{K} \simeq -\frac{2GM}{r^3} + \frac{G^2 M\pi q^2}{r_o^2 r^3} - \frac{3GM\omega_e^2}{r^3\omega_\infty^2} + \frac{3G^2 M\pi q^2\omega_e^2}{r_o^2 r^3\omega_\infty^2} + \mathcal{O}(M^2, q^4). \tag{34}$$

Preprints (www.preprints.org) | NOT PEER-REVIEWED | Posted: 5 July 2022 doi:10.20944/preprints202202.0245.v2

Using GBT we find the bending angle for electric BH to relate it with non-plasma medium. To compute weak-field area, we apply the straight line approximation and that $r(t) = b/\sin\varphi$ at zeroth order

$$\alpha = -\int_0^{\pi}\int_{b/\sin\varphi}^{\infty} \mathcal{K} dS. \tag{35}$$

Hence, the bending angle of light is calculated as

$$\alpha \simeq \frac{4GM}{b} + \frac{G^2 M\pi q^2}{r_o^2 b} + \frac{2GM\omega_e^2}{b\ \omega_\infty^2} - \frac{G^2 M\pi q^2\omega_e^2}{2r_o^2 b\omega_\infty^2} + \mathcal{O}(M^2, q^4). \tag{36}$$

The obtained bending angle (36) depends on the electric charge q, mass of the BH, parameter r_o and impact parameter b. We also observe that the bending angle α of electric BH in plasma medium reduces into Schwarzschild BH bending angle in plasma medium upto the order one of M if we neglect the electric charge q. It is also to be mention here that the bending angle obtained in case of plasma medium (36) reduces to the bending angle obtained in the non-plasma medium (20) by neglecting the plasma terms.

B. Optical Metric and Bending Angle for Magnetic Black Hole

The refractive index in case of magnetic BH is

$$n(r) = \sqrt{1 - \frac{\omega_e^2}{\omega_\infty^2}\left(1 - \frac{2GM}{r} + \frac{p^2 G}{r^2} - \beta\frac{Gp^4}{60r^6}\right)}, \tag{37}$$

where ω_e denotes electron plasma frequency and ω_∞ represents light frequency computed by the spectator at infinity. The corresponding metric in optical space characterized as

$$dt^2 = g_{lm}^{opt} dx^l dx^m = n^2\left[\frac{dr^2}{f^2(r)} + \frac{r^2 d\varphi^2}{f(r)}\right]. \tag{38}$$

The Gaussian curvature is obtained by using Christoffel symbols can be written as

$$\mathcal{K} = \frac{R_{r\varphi r\varphi}(g^{opt})}{det(g^{opt})}. \tag{39}$$

Using Eq.(39), the Gaussian curvature for the magnetic BH in case of plasma medium is determined as

$$\mathcal{K} \simeq -\frac{2GM}{r^3} + \frac{3Gp^2}{r^4} - \beta\frac{7Gp^4}{20r^8} - \frac{3GM\omega_e^2}{r^3\omega_\infty^2} + \frac{5Gp^2\omega_e^2}{r^4\omega_\infty^2} - \beta\frac{13Gp^4\omega_e^2}{20r^8\omega_\infty^2} + \mathcal{O}(G^2, M^2). \tag{40}$$

Preprints (www.preprints.org) | NOT PEER-REVIEWED | Posted: 5 July 2022 doi:10.20944/preprints202202.0245.v2

Using GBT we check the bending angle of magnetic BH to contrast it with non-plasma medium. Along these lines, for getting the point in the weak bending limit, as the light emission seeks after a straight line estimation so by using an instance of $r = b/\sin\varphi$ at zeroth order

$$\alpha = -\int_0^{\pi}\int_{b/\sin\varphi}^{\infty} \mathcal{K} dS. \tag{41}$$

Using the value of $\mathcal{K}$ in (41) the bending angle for the magnetic BH in plasma medium is computed as

$$\alpha \simeq \frac{4GM}{b} - \frac{3Gp^2\pi}{4b^2} + \beta\frac{7Gp^4\pi}{384b^6} + \frac{2GM\omega_e^2}{b\omega_\infty^2} - \frac{Gp^2\pi\omega_e^2}{2b^2\omega_\infty^2} + \beta\frac{Gp^4\pi\omega_e^2}{64b^6\omega_\infty^2} + \mathcal{O}(G^2, M^2). \tag{42}$$

The obtained bending angle (42) depends on the magnetic charge p, mass of the black hole, parameter β and impact parameter b. We also observe that the bending angle α of magnetic BH in plasma medium reduces to Schwarzschild BH bending angle in plasma medium upto the order one of M if we neglect the magnetic charge q. We also observe that the bending angle (42) obtained for magnetic BH in plasma medium reduces to the bending angle (26) obtained in case of non-plasma medium (26), when $\frac{\omega_e^2}{\omega_\infty^2} \to 0$.

V. GRAPHICAL ANALYSIS OF BENDING ANGLES IN PLASMA MEDIUM

This section is devoted to the study of the behaviour of bending angles of electric and magnetic BHs in plasma medium graphically and to explain the influence of plasma, electric charge q, impact parameter b and parameter r_o (in case of electric BH) and magnetic charge p, impact parameter b and the parameter β (in case of magnetic BH) on the deflection angles.

Preprints (www.preprints.org) | NOT PEER-REVIEWED | Posted: 5 July 2022 doi:10.20944/preprints202202.0245.v2

A. For electric Black Hole

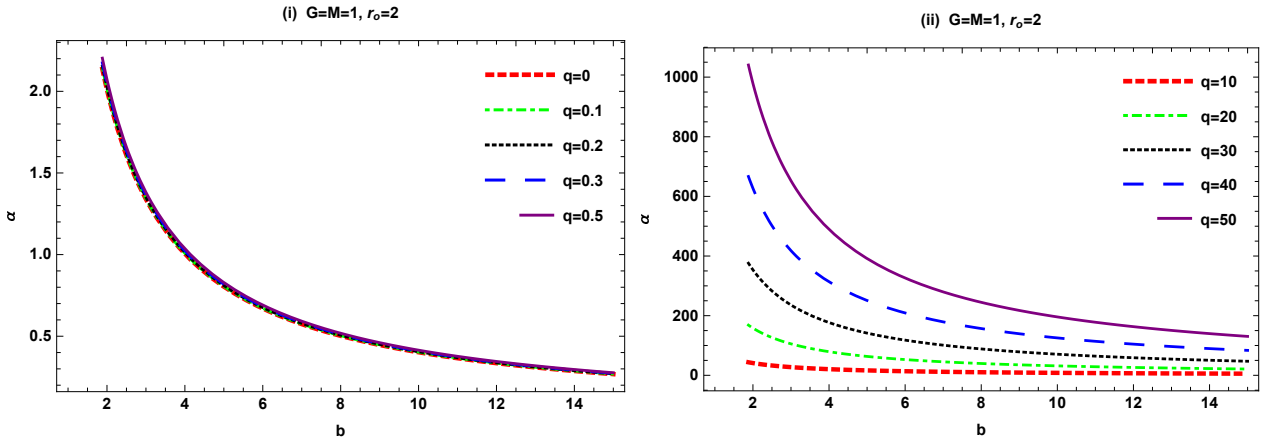

Figure 7: α versus b.

- **Figure 7** demonstrates the graphical behaviour of the bending angle α of electric BH with respect to the impact parameter b for $\frac{\omega_e^2}{\omega_\infty^2} = 0.1$ and fixed values of M, G, r_o.

  (i) For the small values of q graph between the the bending angle α and the impact parameter b shows that the behaviour of the bending angle α is uniformly constant.

  (ii) For the large values of q graph between the the bending angle α and the impact parameter b depicts that the behaviour of the bending angle α is increasing gradually.

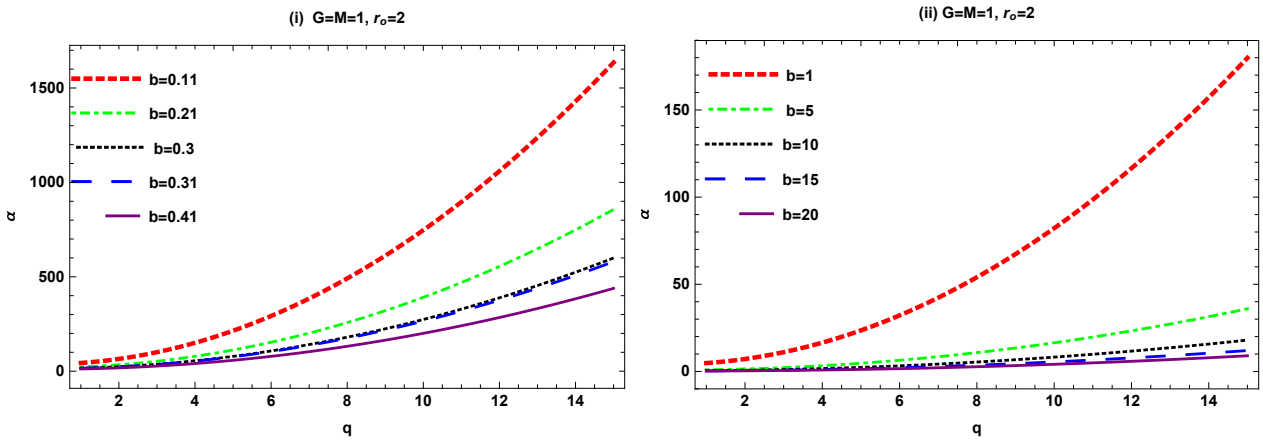

Figure 8: α versus q.

- **Figure 8** demonstrates the graphical behaviour of bending angle α of magnetic BH with respect to the electric charge q for $\frac{\omega_e^2}{\omega_\infty^2} = 0.1$ and fixed values of M, G, r_o .

Preprints (www.preprints.org) | NOT PEER-REVIEWED | Posted: 5 July 2022 doi:10.20944/preprints202202.0245.v2

(i) For the small values of impact parameter b the graph of bending angle α with respect to electric charge q exhibits that the bending angle α shows decreasing behaviour.

(ii) For the large values of b the graph of bending angle α with respect to electric charge q shows that for the values of $1 < b < 5$ the bending angle α increasing but as the value of impact parameter b increasing the bending angle α starts decreasing.

B. For Magnetic Black Hole

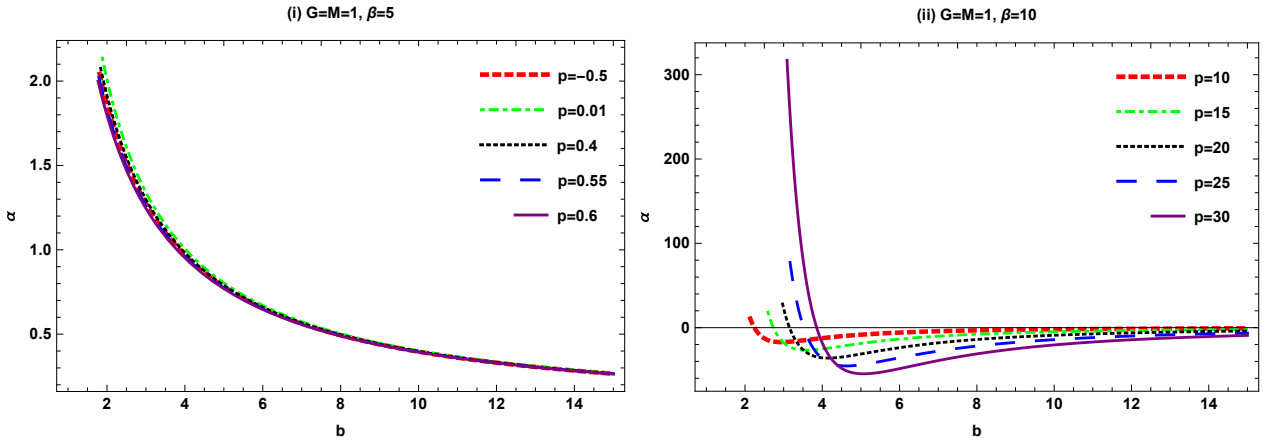

Figure 9: α versus b.

- **Figure 9** exhibits the graphical behaviour of bending angle α of magnetic BH with respect to the impact parameter b for $\frac{\omega_e^2}{\omega_\infty^2} = 0.1$ and fixed values of M, G,β.

  (i) Graph between bending angle α and impact parameter b shows that for the very small variation of magnetic charge p and parameter $\beta = 5$ the bending angle α rapidly decreases.

  (ii) Graph between bending angle α and impact parameter b depicts that for the large value of magnetic charge p and parameter $\beta = 10$, the bending angle α increasing and then goes to infinity.

Preprints (www.preprints.org) | NOT PEER-REVIEWED | Posted: 5 July 2022 doi:10.20944/preprints202202.0245.v2

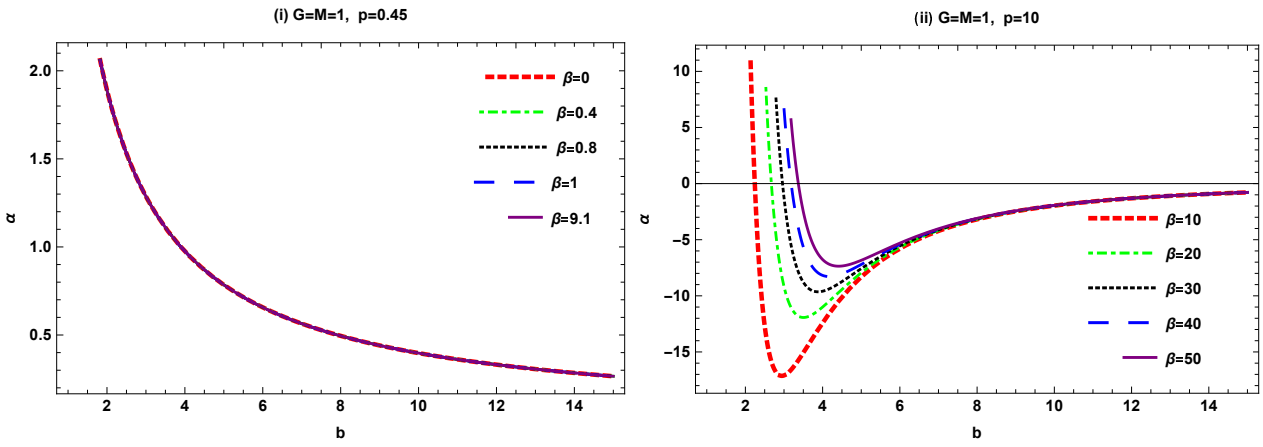

Figure 10: α versus b.

- **Figure 10** represents the graphical behaviour of bending angle α of magnetic BH with respect to the impact parameter b and for $\frac{\omega_e^2}{\omega_\infty^2} = 0.1$ and fixed values of magnetic charge p, G, M.

  (i) Graph between the bending angle α and impact parameter b exhibits that for small values of parameter β and magnetic charge $p = 0.45$ the bending angle α is decreasing constantly.

  (ii) Graph between the bending angle α and impact parameter b exhibits that for the large values of parameter β and magnetic charge $p = 10$ the bending angle α firstly starts decreasing negatively and then increasing and goes to the infinity.

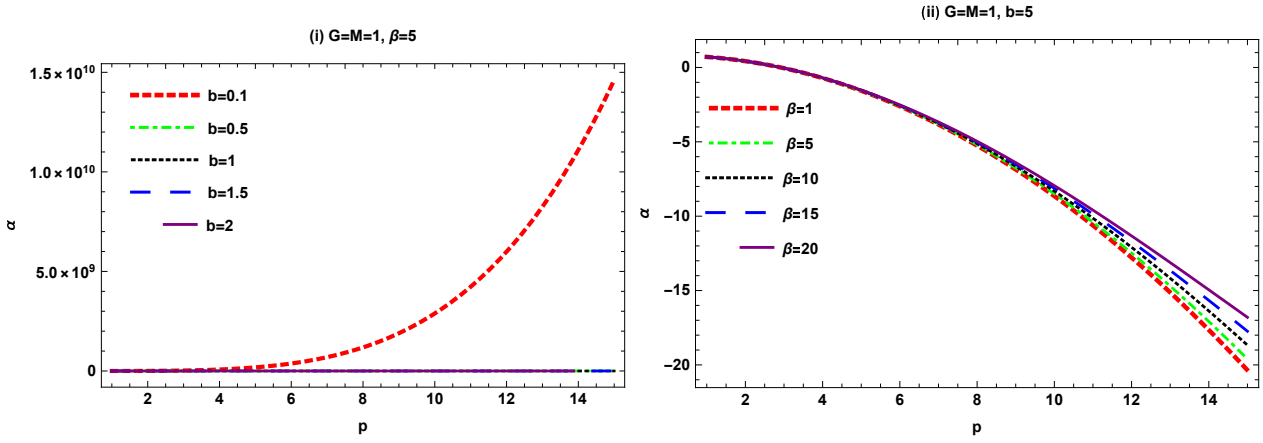

Figure 11: α versus p.

- **Figure 11** demonstrates the graphical behaviour of bending angle α of magnetic BH with respect to the magnetic charge p for $\frac{\omega_e^2}{\omega_\infty^2} = 0.1$ and fixed values of G, M.

Preprints (www.preprints.org) | NOT PEER-REVIEWED | Posted: 5 July 2022 doi:10.20944/preprints202202.0245.v2

(i) Graph between the bending angle α and magnetic charge p shows that for the variation of impact parameter b and parameter $\beta = 5$ firstly bending angle α increases then start decreasing.

(ii) Graph between the bending angle α and magnetic charge p for the variation in the value of β and impact parameter $b = 5$ shows that the bending angle α negatively increasing.

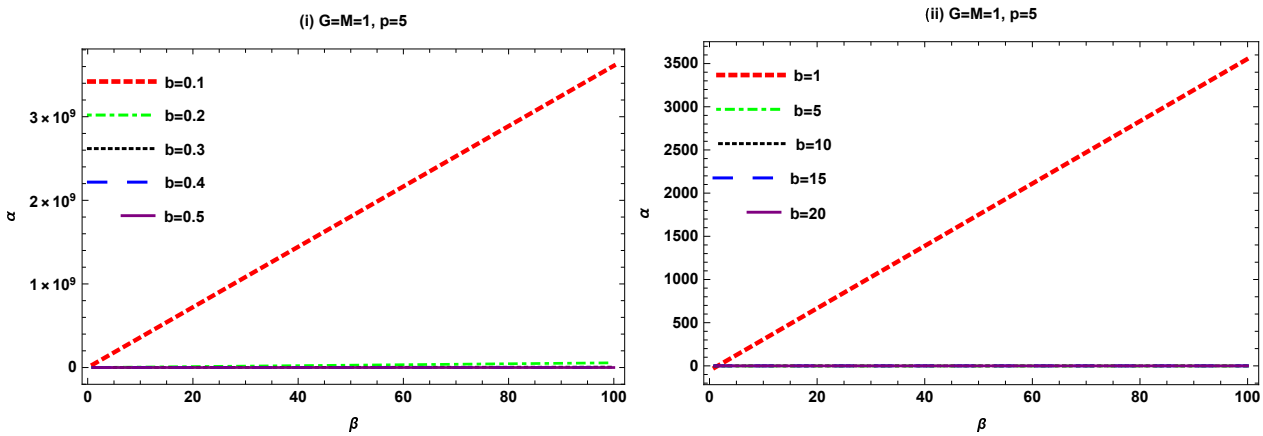

Figure 12: α versus β.

- **Figure 12** represents the graphical behaviour of bending angle α of magnetic BH with respect to the β for $\frac{\omega_e^2}{\omega_\infty^2} = 0.1$ and fixed values of magnetic charge p, G and M.

  (i) Graph between the bending angle α and β exhibits that for the small variation of the impact parameter b and magnetic charge $p = 5$ bending angle α is decreasing.

  (ii) Graph between the bending angle α and β for the large value of impact parameter b and magnetic charge $p = 5$ shows that the bending angle α is decreasing.

VI. GREYBODY FACTOR FOR ELECTRIC AND MAGNETIC BLACK HOLES

In this part, we work out for the bound of greybody factor for the electric and magnetic BHs. There are numerous strategies to figure the greybody variable like matching teachnique and WKB approximation [88]. In this current work, we will consider the technique that doesn't utilize such approximations, for example, rigorous lower bound on the greybody factor [89]-[97].

Preprints (www.preprints.org) | NOT PEER-REVIEWED | Posted: 5 July 2022 doi:10.20944/preprints202202.0245.v2

A. For Electric Black Hole

The spherically symmetric and static form of a line-element defined by Eq.(4), where the metric function for the electric BH is

$$f(r) = 1 - \frac{2GM}{r} - \frac{\pi q^2 G}{2r_o^2} + \mathcal{O}(r^2 lnr). \tag{43}$$

The event horizon is obtained by taking $f(r) = 0$, we get

$$r_h = \frac{4r_o^2 GM}{2r_o^2 - G\pi q^2}. \tag{44}$$

The Schrodinger-like equation is demonstrated as

$$\left(\frac{d^2}{dr_*^2} + \omega^2 - \breve{\breve{V}}(r)\right)\psi = 0, \tag{45}$$

where, $dr_*^2 = \frac{1}{f(r)}dr$ and r_* represents the "tortoise coordinate" and $\breve{\breve{V}}(r)$ indicates the potential which is given by

$$\breve{\breve{V}}(r) = \frac{f(r)f'(r)}{r} + l(l+1)\frac{f(r)}{r^2}. \tag{46}$$

For $h = \omega$, the lower bound on the transmission probability is defined as [91]

$$T \geq \frac{1}{\cosh^2}\left(\frac{1}{2\omega}\int_{r_h}^{\infty}\frac{\breve{\breve{V}}(r)}{f(r)}dr\right). \tag{47}$$

Using the value of $\breve{\breve{V}}(r)$ in Eq.(47) we get the following expressions

$$= \frac{1}{\cosh^2}\left[\frac{1}{2\omega}\int_{r_h}^{\infty}\left(\frac{f'(r)}{r} + \frac{l(l+1)}{r^2}\right)dr\right], \tag{48}$$

$$= \frac{1}{\cosh^2}\left[\frac{1}{2\omega}\left(\frac{GM}{r_h^2} + \frac{l(l+1)}{r_h}\right)\right]. \tag{49}$$

Substituting the value of r_h in Eq.(49), we attain the bound as

$$T \geq \frac{1}{\cosh^2}\left[\frac{1}{2\omega}\left(\frac{(G\pi q^2 - 2r_o^2)^2}{16r_o^4 GM} - \frac{l(l+1)(G\pi q^2 - 2r_o^2)}{4r_o^2 GM}\right)\right]. \tag{50}$$

The above equation represents the lower bound for the greybody factor of electric charge BH which depends on the mass of the BH, r_o and the electric charge q of the BH. In the absence of the electric charge q, the above bound reduces to the form

$$T \geq \frac{1}{\cosh^2}\left[\frac{2l(l+1)+1}{8\omega GM}\right], \tag{51}$$

which is the lower bound of the Schwarzschild BH [91].

Preprints (www.preprints.org) | NOT PEER-REVIEWED | Posted: 5 July 2022 doi:10.20944/preprints202202.0245.v2

B. For Magnetic Black Hole

The spherically symmetric form of a metric is defined in Eq.(4), where the metric function for the magnetic BH is [120]:

$$f(r) = 1 - \frac{2GM}{r} + \frac{p^2 G}{r^2} - \beta \frac{Gp^4}{60r^6} + \mathcal{O}(r^{-10}). \tag{52}$$

The event horizon for the magnetic BH can not be calculated numerically, so in our analysis we calculated it graphically. For this we plot the graph between metric function $f(r)$ and r-coordinate by keeping parameter β and magnetic charge p fixed.

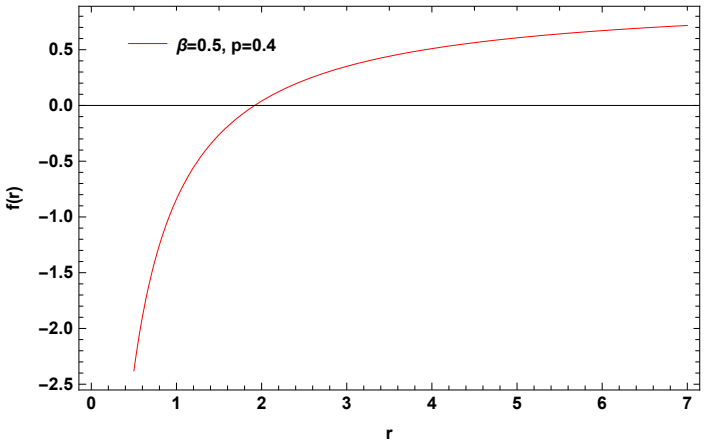

Figure 13: $f(r)$ versus r.

From figure 13, we get $r = 1.8$ and the value of event horizon $r_h = \frac{1}{r} = 0.555$. Now by using the Eq.(48), we get

$$T \geq \frac{1}{\cosh^2}\left[\frac{1}{2\omega}\left(\frac{GM}{r_h^2} + \frac{l(l+1)}{r_h} - \frac{2Gp^2}{3r_h^3} + \frac{Gp^4\beta}{70r_h^7}\right)\right]. \tag{53}$$

By putting the value of r_h in (53), we obtain the rigorous bound

$$T \geq \frac{1}{\cosh^2}\left[\frac{3.24649GM - 3.89969Gp^2 + 1.8018l(l+1) + 0.880747Gp^4\beta}{2\omega}\right]. \tag{54}$$

The above equation is the bound for the greybody factor of the magnetic BH which depend on the mass of the BH, magnetic charge p and parameter β.

VII. GRAPHICAL ANALYSIS OF GREYBODY BOUND

This section represents the graphical affects of greybody bound for electric and magnetic BHs and potential (we set $\breve{V}(r) = V(r)$) at the same time as for the distinct values of the charges of BHs with angular momentum $l = 0, 1$ respectively.

Preprints (www.preprints.org) | NOT PEER-REVIEWED | Posted: 5 July 2022 doi:10.20944/preprints202202.0245.v2

A. For Electric Black Hole

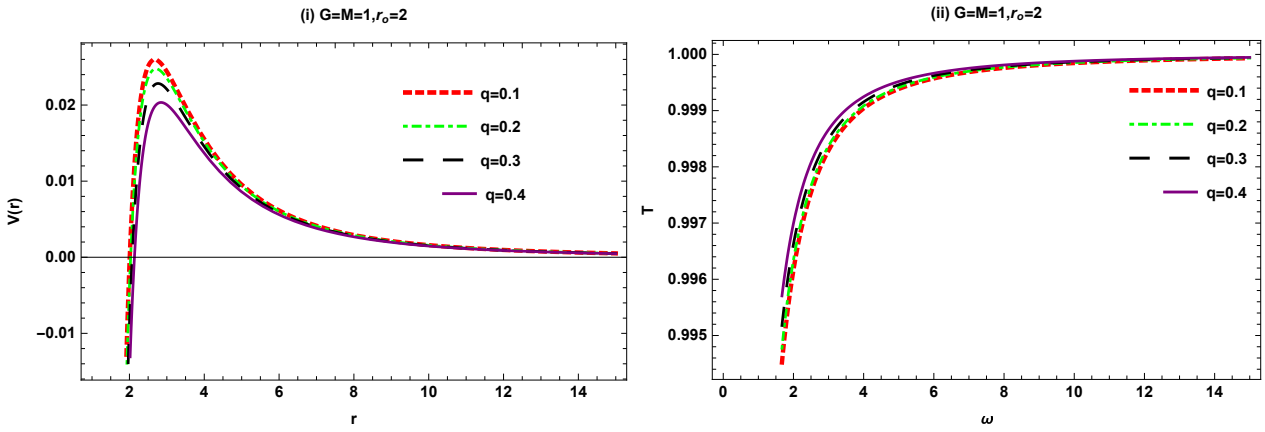

Figure 14: (i) indicates the potential with $l = 0$ and (ii) indicates the corresponding greybody factor bound of electric BH.

- We observe that value of the potential with $l = 0$ increases when the value of the electric charge q decreases and so the bound of the greybody factor becomes lower as it becomes difficult for the wave to transmit through the higher potential.

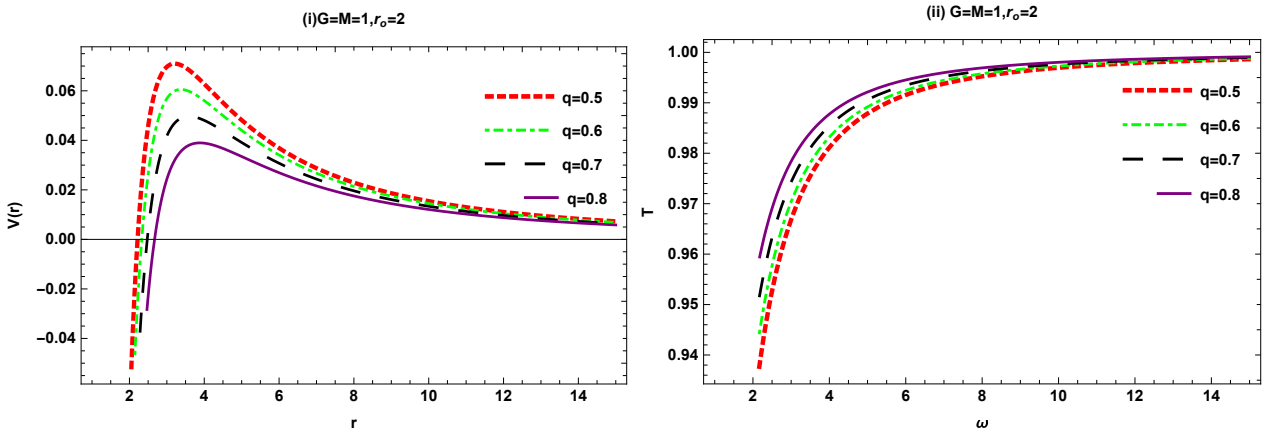

Figure 15: (i) indicates the potential behaviour with $l = 1$ and (ii) indicates the corresponding greybody factor bound of electric BH.

- We analyze that the value of the potential with $l = 1$ starts increasing when the value of the electric charge q decreases and the corresponding bound of the greybody factor becomes lower and it becomes difficult for the wave to transmit through higher potential.

Preprints (www.preprints.org) | NOT PEER-REVIEWED | Posted: 5 July 2022 doi:10.20944/preprints202202.0245.v2

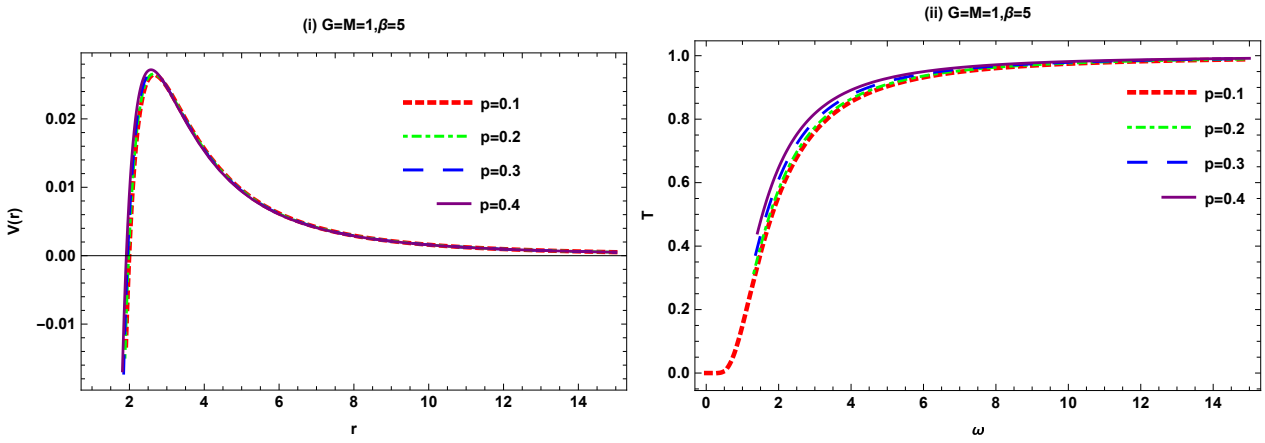

Figure 16: (i) indicates the potential behaviour with $l = 0$ and (ii) indicates the regarding greybody factor bound of magnetic BH.

- We analyze that the value of the potential with $l = 0$ starts increasing when the value of the electric charge q increases and bound of the greybody factor becomes lower and it becomes difficult for the wave to transmit through the high value of the potential.

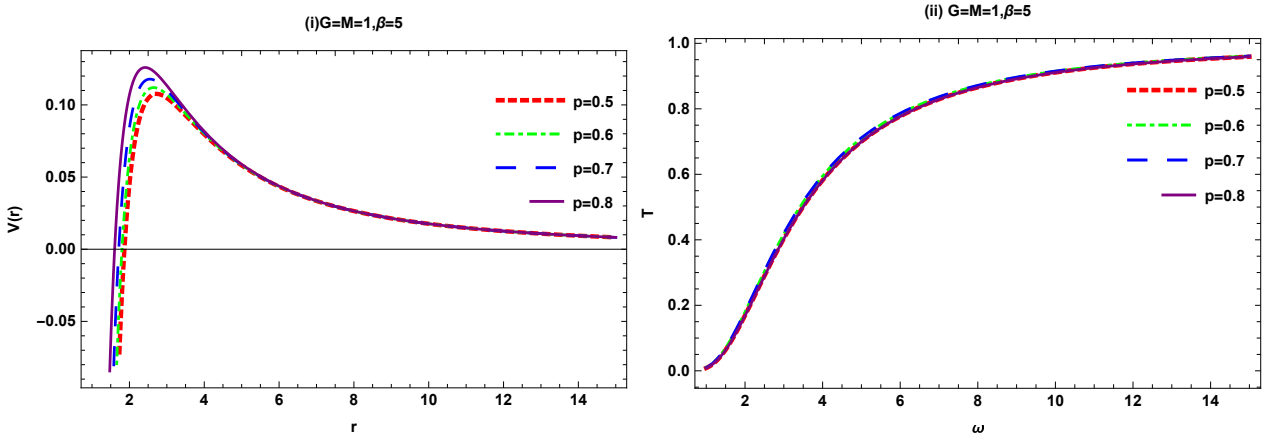

Figure 17: (i) indicates the potential behaviour with $l = 1$ and (ii) indicates the regarding greybody factor bound of magnetic BH.

- We investigate that the potential with $l = 1$ increases as the value of the magnetic charge p increases and the corresponding bound becomes lower and is difficult for the wave to pass through the high value of the potential.

Preprints (www.preprints.org) | NOT PEER-REVIEWED | Posted: 5 July 2022 doi:10.20944/preprints202202.0245.v2

VIII. CONCLUSION

In our analysis, we have analyzed the NLED model to calculate the bending angles in non-plasma and plasma mediums and greybody factor bounds for electric and magnetic BHs. The results are obtained as follows.

1. Bending Angle α

(i) Non-plasma Medium

The bending angles for electric and magnetic BHs are obtained by using the value of $\mathcal{K}$ as follows

$$\alpha \simeq \frac{4GM}{b} + \frac{G^2 M\pi q^2}{r_o^2 b} + \mathcal{O}(M^2, q^4), \tag{55}$$

$$\alpha \simeq \frac{4GM}{b} - \frac{3Gp^2\pi}{4b^2} + \beta\frac{7Gp^4\pi}{384b^6} + \mathcal{O}(G^2, M^2). \tag{56}$$

We observed that the obtained bending angle for electric BH depends on the impact parameter b, mass of the BH, parameter r_o and the electric charge q and for the magnetic BH bending angle depends on the impact parameter b, mass of the BH, β and magnetic charge p. We proved that the bending angles for electric and magnetic BHs reduces to Schwarzschild BH bending angle in non-plasma medium upto the order one of M if we neglect the electric and magnetic charges.

(ii) Plasma Medium

We also discussed the bending angles of these BHs in plasma medium by using the same technique as in non-plasma medium. The Bending angles we have obtained for electric and magnetic BHs in plasma medium respectively as follows

$$\alpha \simeq \frac{4GM}{b} + \frac{G^2 M\pi q^2}{r_o^2 b} + \frac{2GM\omega_e^2}{b\ \omega_\infty^2} - \frac{G^2 M\pi q^2\omega_e^2}{2r_o^2 b\omega_\infty^2} + \mathcal{O}(M^2, q^4). \tag{57}$$

$$\begin{aligned}\alpha \ \simeq\ & \frac{4GM}{b} - \frac{3Gp^2\pi}{4b^2} + \beta\frac{7Gp^4\pi}{384b^6} + \frac{2GM\omega_e^2}{b\omega_\infty^2} - \frac{Gp^2\pi\omega_e^2}{2b^2\omega_\infty^2} \\ &+\ \beta\frac{Gp^4\pi\omega_e^2}{64b^6\omega_\infty^2} + \mathcal{O}(G^2, M^2).\end{aligned} \tag{58}$$

We have investigated that the obtained bending angle α for electric BH depends on the impact parameter b, mass of the BH, parameter r_o and the electric charge q of the BH and for magnetic BH depends on the impact parameter b, mass of the BH, parameter β and magnetic charge p. We proved that the bending angles for electric and magnetic BHs reduces to Schwarzschild BH bending angle in non-plasma medium upto the order one of M if we neglect the electric and

Preprints (www.preprints.org) | NOT PEER-REVIEWED | Posted: 5 July 2022 doi:10.20944/preprints202202.0245.v2

magnetic BHs charges. If we remove the plasma effect then the bending angles in plasma medium reduces to the bending angles for both electric and magnetic BHs in non-plasma medium.

2. Graphically

After computing the bending angles, we also analyzed the graphical behaviour of the bending angles for both electric and magnetic charged BHs in both non-plasma and plasma mediums. We also observed that the graphical behaviour exhibits similar results in both non-plasma and plasma mediums. These results are described as follows

(i) For Electric Black Hole

- **Bending angle α versus impact parameter b**:

  For the fixed values of $G = M = 1$ and $r_o = 2$, for the small values of q bending angle α is uniformly constant and for the large values of q bending angle α is increasing gradually.

- **Bending angle α versus electric charge q**:

  For the fixed values of $G = M = 1$ and $r_o = 2$, for the small values of b bending angle α is decreasing and for the large values of b bending angle α firslty increasing and then start decreasing.

(ii) For Magnetic Black Hole

- **Bending angle α versus impact parameter b**:

  For the small values of p ($G = M = 1$ and $\beta = 5$) bending angle α is rapidly decreasing and for the large values of p ($G = M = 1$ and $\beta = 10$) bending angle α is decreasing and then goes to infinity. For the small values of β ($G = M = 1$ and $p = 0.45$) bending angle α is constantly decreasing and for the large values of β ($G = M = 1$ and $p = 10$) bending angle α is decreasing negatively and then increasing goes to infinity.

- **Bending angle α versus magnetic charge p**:

  For the small values of b ($G = M = 1$ and $\beta = 5$) firstly the bending angle α is increasing and the start decreasing and for the large values of β ($G = M = 1$ and $b = 5$) bending angle α is negatively increasing.

Preprints (www.preprints.org) | NOT PEER-REVIEWED | Posted: 5 July 2022 doi:10.20944/preprints202202.0245.v2

- **Bending angle α versus parameter β:**

  For the fixed values of $G = M = 1$ and $p = 5$, for the small values of b bending angle α is decreasing and for the large values of b, bending angle α also shows the decreasing behaviour.

3. Greybody Factor Bounds T

We calculated the greybody factor bounds for both electric and magnetic BHs. In order to obtain the greybody bounds, we graphically determined the horizon for magnetic BH and for electric BH we calculate the horizon numerically.

(i) For Electric Black Hole

The bound on the greybody factor in the case of electric BH obtained as

$$T \geq \frac{1}{\cosh^2}\left[\frac{1}{2\omega}\left(\frac{(G\pi q^2-2r_o^2)^2}{16r_o^4GM}-\frac{l(l+1)(G\pi q^2-2r_o^2)}{4r_o^2GM}\right)\right]. \tag{59}$$

The obtained bound for the greybody factor of the electric BH depends on the mass of the BH, r_o and the electric charge q of the BH. While in the absence of the electric charge q, the above bound for the electric BH reduces into the form

$$T \geq \frac{1}{\cosh^2}\left[\frac{2l(l+1)+1}{8\omega GM}\right], \tag{60}$$

which is the lower bound on the greybody factor of the Schwarzschild BH.

(ii) For Magnetic Black Hole

In the case of magnetic BH, the derived bound on the greybody factor is defined as follows

$$T \geq \frac{1}{\cosh^2}\left[\frac{3.24649GM-3.89969Gp^2+1.8018l(l+1)+0.880747Gp^4\beta}{2\omega}\right]. \tag{61}$$

The bound for the greybody factor of magnetic BH depend on the mass of the BH, magnetic charge p and parameter β.

4. Graphical Analysis of Greybody Bound

At the end, we investigated the graphical results of the greybody bounds for different values of electric and magnetic charges. We noticed that the greybody bound relies on the greatest worth of the potential. We have analyzed that for the small value of electric charge q of electric BH, the value of the potential increases and the bound decreases. In case of magnetic BH, the potential

increases as the value of the magnetic charge p increases and the value of the bound decreases and it becomes difficult for the waves to passed through the highest potential.

---

[1] K. Akiyama *et al.* [Event Horizon Telescope], Astrophys. J. Lett. **875**, L1 (2019).

[2] P. V. P. Cunha and C. A. R. Herdeiro, Gen. Rel. Grav. **50**, no.4, 42 (2018).

[3] J. Soldner, Ueber die Ablenkung eines Lichtstrals von seiner geradlinigen Bewegung, durch die Attraktion eines Weltkörpers, an welchem er nahe vorbei geht. Berliner Astronomisches Jahrbuch,161-172.cc (1804).

[4] A. Einstein, Science **84**, 506-507 (1936).

[5] C. A. R. Herdeiro and J. P. S. Lemos, [arXiv:1811.06587 [physics.hist-ph]].

[6] B. P. Abbott *et al.* [LIGO Scientific and Virgo], Phys. Rev. Lett. **116**, no.13, 131103 (2016).

[7] M. Bartelmann and P. Schneider, Phys. Rept. **340**, 291-472 (2001).

[8] E. F. Eiroa, G. E. Romero and D. F. Torres, Phys. Rev. D **66**, 024010 (2002).

[9] C. R. Keeton, C. S. Kochanek and E. E. Falco, Astrophys. J. **509**, 561-578 (1998).

[10] M. Sharif and S. Iftikhar, Astrophys. Space Sci. **361**, no.1, 36 (2016).

[11] K. S. Virbhadra, D. Narasimha and S. M. Chitre, Astron. Astrophys. **337**, 1-8 (1998).

[12] A. F. Zakharov, Int. J. Mod. Phys. D **27**, no.06, 1841009 (2018).

[13] K. S. Virbhadra and G. F. R. Ellis, Phys. Rev. D **65**, 103004 (2002).

[14] K. S. Virbhadra and G. F. R. Ellis, Phys. Rev. D 62, 084003 (2000).

[15] K. S. Virbhadra, Phys. Rev. D 79, 083004 (2009).

[16] R. Shaikh, P. Kocherlakota, R. Narayan and P. S. Joshi, Mon. Not. Roy. Astron. Soc. **482**, no.1, 52-64 (2019).

[17] S. U. Islam, R. Kumar and S. G. Ghosh, JCAP **09**, 030 (2020)

[18] R. Kumar, S. G. Ghosh and A. Wang, Phys. Rev. D **101**, no.10, 104001 (2020)

[19] T. Manna, F. Rahaman, S. Molla, J. Bhadra and H. H. Shah, Gen. Rel. Grav. **50**, no.5, 54 (2018).

[20] P. K. F. Kuhfittig, Eur. Phys. J. C **74**, no.99, 2818 (2014).

[21] F. Rahaman, M. Kalam and S. Chakraborty, Chin. J. Phys. **45**, 518 (2007).

[22] G. W. Gibbons and M. C. Werner, Class. Quant. Grav. **25**, 235009 (2008).

[23] M. C. Werner, Gen. Rel. Grav. **44**, 3047-3057 (2012).

[24] G. Crisnejo and E. Gallo, Phys. Rev. D **97**, no.12, 124016 (2018).

 doi:10.20944/preprints202202.0245.v2

[25] A. Ishihara, Y. Suzuki, T. Ono, T. Kitamura and H. Asada, Phys. Rev. D **94**, no.8, 084015 (2016)

[26] A. Ishihara, Y. Suzuki, T. Ono and H. Asada, Phys. Rev. D **95**, no.4, 044017 (2017).

[27] A. Övgün, Phys. Rev. D **98**, no.4, 044033 (2018).

[28] A. Övgün, Phys. Rev. D **99**, no.10, 104075 (2019).

[29] A. Övgün, Universe **5**, no.5, 115 (2019).

[30] K. Jusufi, M. C. Werner, A. Banerjee and A. Övgün, Phys. Rev. D **95**, no.10, 104012 (2017).

[31] K. de Leon and I. Vega, Phys. Rev. D **99**, no.12, 124007 (2019).

[32] K. Jusufi and A. Övgün, Phys. Rev. D **97**, no.2, 024042 (2018).

[33] T. Ono, A. Ishihara and H. Asada, Phys. Rev. D **96**, no.10, 104037 (2017)

[34] K. Jusufi, A. Ovgün and A. Banerjee, Phys. Rev. D **96**, no.8, 084036 (2017).

[35] A. Övgün, G. Gyulchev and K. Jusufi, Annals Phys. **406**, 152-172 (2019).

[36] H. Arakida, Gen. Rel. Grav. **50**, no.5, 48 (2018).

[37] K. Jusufi and A. Ovgün, Phys. Rev. D **97**, no.6, 064030 (2018).

[38] T. Ono, A. Ishihara and H. Asada, Phys. Rev. D **98**, no.4, 044047 (2018).

[39] K. Jusufi, A. Övgün, J. Saavedra, Y. Vásquez and P. A. González, Phys. Rev. D **97**, no.12, 124024 (2018).

[40] T. Ono, A. Ishihara and H. Asada, Phys. Rev. D **99**, no.12, 124030 (2019).

[41] W. Javed, R. Babar and A. Övgün, Phys. Rev. D **99**, no.8, 084012 (2019).

[42] K. Jafarzade, M. Kord Zangeneh and F. S. N. Lobo, JCAP **04**, 008 (2021).

[43] K. Takizawa, T. Ono and H. Asada, Phys. Rev. D **101**, no.10, 104032 (2020).

[44] Y. Kumaran and A. Övgün, Chin. Phys. C **44**, no.2, 025101 (2020).

[45] Z. Li and A. Övgün, Phys. Rev. D **101**, no.2, 024040 (2020).

[46] Z. Li, G. Zhang and A. Övgün, Phys. Rev. D **101**, no.12, 124058 (2020).

[47] A. Övgün, Turk. J. Phys. **44**, no.5, 465-471 (2020).

[48] Y. Kumaran and A. Övgün, Turk. J. Phys. **45**, 247-267 (2021).

[49] M. Okyay and A. Övgün, JCAP **01**, no.01, 009 (2022).

[50] R. C. Pantig and A. Övgün, Eur. Phys. J. C **82**, no.5, 391 (2022).

[51] H. El Moumni, K. Masmar and A. Övgün, Int. J. Geom. Meth. Mod. Phys. **19**, no.06, 2250094 (2022).

[52] A. Belhaj, H. Belmahi, M. Benali and H. El Moumni, Int. J. Mod. Phys. D **31**, no.07, 2250054 (2022).

 doi:10.20944/preprints202202.0245.v2

[53] A. Belhaj, M. Benali, A. El Balali, H. El Moumni and S. E. Ennadifi, Class. Quant. Grav. **37**, no.21, 215004 (2020).

[54] R. C. Pantig and A. Övgün, [arXiv:2202.07404 [astro-ph.GA]].

[55] A. Uniyal, R. C. Pantig and A. Övgün, [arXiv:2205.11072 [gr-qc]].

[56] R. C. Pantig and A. Övgün, [arXiv:2206.02161 [gr-qc]].

[57] J. Rayimbaev, R. C. Pantig, A. Övgün, A. Abdujabbarov and D. Demir, [arXiv:2206.06599 [gr-qc]].

[58] R. C. Pantig, P. K. Yu, E. T. Rodulfo and A. Övgün, Annals of Physics 436, 168722 (2022).

[59] K. Jusufi, F. Rahaman and A. Banerjee, Annals Phys. **389**, 219-233 (2018).

[60] F. Rahaman, M. Kalam and S. Chakraborty, Chin. J. Phys. **45**, 518 (2007).

[61] P. K. F. Kuhfittig, Eur. Phys. J. C **74**, no.99, 2818 (2014).

[62] K. Takizawa, T. Ono and H. Asada, Phys. Rev. D **102**, no.6, 064060 (2020).

[63] T. Ono and H. Asada, Universe **5**, no.11, 218 (2019).

[64] Q. M. Fu, L. Zhao and Y. X. Liu, Phys. Rev. D **104**, no.2, 024033 (2021).

[65] H. El Moumni, K. Masmar and A. Övgün, [arXiv:2008.06711 [gr-qc]].

[66] W. Javed, R. Babar and A. Övgün, Phys. Rev. D **100**, no.10, 104032 (2019).

[67] W. Javed, J. Abbas and A. Övgün, Eur. Phys. J. C **79**, no.8, 694 (2019).

[68] W. Javed, J. Abbas and A. Övgün, Phys. Rev. D **100**, no.4, 044052 (2019).

[69] W. Javed, A. Hamza and A. Övgün, Phys. Rev. D **101**, no.10, 103521 (2020).

[70] W. Javed, M. B. Khadim, A. Övgün and J. Abbas, Eur. Phys. J. Plus **135**, no.3, 314 (2020).

[71] W. Javed, M. B. Khadim and A. Övgün, Eur. Phys. J. Plus **135**, no.7, 595 (2020).

[72] W. Javed, A. Hamza and A. Övgün, Mod. Phys. Lett. A **35**, no.39, 2050322 (2020).

[73] W. Javed, A. Hamza and A. Övgün, Universe **7**, no.10, 385 (2021).

[74] W. Javed, J. Abbas, Y. Kumaran and A. Övgün, Int. J. Geom. Meth. Mod. Phys. **18**, no.01, 2150003 (2021).

[75] W. Javed, J. Abbas and A. Övgün, Annals Phys. **418**, 168183 (2020).

[76] S. Hensh, A. Abdujabbarov, J. Schee and Z. Stuchlík, Eur. Phys. J. C **79**, no.6, 533 (2019).

[77] S. W. Hawking, Commun. Math. Phys. **43**, 199-220 (1975) [erratum: Commun. Math. Phys. **46**, 206 (1976)].

[78] S. Fernando, Gen. Rel. Grav. **37**, 461-481 (2005).

[79] G. Panotopoulos and A. Rincón, Phys. Rev. D **97**, no.8, 085014 (2018).

[80] J. M. Maldacena and A. Strominger, Phys. Rev. D **55**, 861-870 (1997).

[81] D. Ida, K. y. Oda and S. C. Park, Phys. Rev. D **67**, 064025 (2003) [erratum: Phys. Rev. D **69**, 049901 (2004)].

[82] M. Cvetic and F. Larsen, Phys. Rev. D **56**, 4994-5007 (1997).

[83] T. Harmark, J. Natario and R. Schiappa, Adv. Theor. Math. Phys. **14**, no.3, 727-794 (2010).

[84] S. S. Gubser and I. R. Klebanov, Phys. Rev. Lett. **77**, 4491-4494 (1996).

[85] I. R. Klebanov and S. D. Mathur, Nucl. Phys. B **500**, 115-132 (1997).

[86] H. W. Lee and Y. S. Myung, Phys. Rev. D **58**, 104013 (1998).

[87] S. Chen and J. Jing, Phys. Lett. B **691**, 254-260 (2010).

[88] R. A. Konoplya and A. F. Zinhailo, Phys. Lett. B **810**, 135793 (2020).

[89] P. Boonserm and M. Visser, Annals Phys. **323**, 2779-2798 (2008).

[90] P. Boonserm, [arXiv:0907.0045 [math-ph]].

[91] P. Boonserm and M. Visser, Phys. Rev. D **78**, 101502 (2008).

[92] T. Ngampitipan and P. Boonserm, Int. J. Mod. Phys. D **22**, 1350058 (2013).

[93] P. Boonserm, T. Ngampitipan and P. Wongjun, Eur. Phys. J. C **78**, no.6, 492 (2018).

[94] P. Boonserm, T. Ngampitipan and M. Visser, JHEP **03**, 113 (2014).

[95] P. Boonserm, A. Chatrabhuti, T. Ngampitipan and M. Visser, J. Math. Phys. **55**, 112502 (2014).

[96] T. Ngampitipan and P. Boonserm, J. Phys. Conf. Ser. **435**, 012027 (2013).

[97] P. Boonserm, T. Ngampitipan and P. Wongjun, Eur. Phys. J. C **79**, no.4, 330 (2019).

[98] A. Övgün, Eur. Phys. J. C **77**, no.2, 105 (2017).

[99] A. Övgün, G. Leon, J. Magaña and K. Jusufi, Eur. Phys. J. C **78**, no.6, 462 (2018).

[100] D. P. Sorokin, [arXiv:2112.12118 [hep-th]].

[101] H. B. Benaoum and A. Ovgun, Class. Quant. Grav. **38**, no.13, 135019 (2021).

[102] P. Sarkar, P. Kumar Das and G. C. Samanta, Phys. Scripta **96**, no.6, 065305 (2021).

[103] G. Otalora, A. Övgün, J. Saavedra and N. Videla, JCAP **06**, 003 (2018).

[104] S. H. Mazharimousavi and M. Halilsoy, Annalen Phys. **531**, no.12, 1900236 (2019).

[105] S. I. Kruglov, Int. J. Mod. Phys. A **32**, no.23n24, 1750147 (2017)

[106] S. I. Kruglov, Universe **4**, no.5, 66 (2018)

[107] S. I. Kruglov, Annals Phys. **378**, 59-70 (2017).

[108] M. S. Rad, S. H. Hendi, K. Matsuno and A. Sheykhi, Annals Phys. **363**, 485-495 (2015)

[109] E. Ayon-Beato and A. Garcia, Phys. Rev. Lett. **80**, 5056-5059 (1998).

[110] K. A. Bronnikov, Phys. Rev. D **63**, 044005 (2001).

 doi:10.20944/preprints202202.0245.v2

[111] E. Ayon-Beato and A. Garcia, Phys. Lett. B **493**, 149-152 (2000).

[112] E. Ayon-Beato and A. Garcia, Phys. Lett. B **464**, 25 (1999).

[113] S. A. Hayward, Phys. Rev. Lett. **96**, 031103 (2006).

[114] S. Ansoldi, P. Nicolini, A. Smailagic and E. Spallucci, Phys. Lett. B **645**, 261-266 (2007).

[115] C. Bambi and L. Modesto, Phys. Lett. B **721**, 329-334 (2013).

[116] B. Toshmatov, B. Ahmedov, A. Abdujabbarov and Z. Stuchlik, Phys. Rev. D **89**, no.10, 104017 (2014).

[117] J. P. S. Lemos and V. T. Zanchin, Phys. Rev. D **83**, 124005 (2011).

[118] G. J. Olmo and D. Rubiera-Garcia, Phys. Rev. D **84**, 124059 (2011).

[119] V. P. Frolov, Phys. Rev. D **94**, no.10, 104056 (2016)

[120] S. H. Mazharimousavi and M. Halilsoy, Annals Phys. **433**, 168579 (2021).

[121] M. Born and L. Infeld, Proc. Roy. Soc. Lond. A **144**, no.852, 425-451 (1934).